# Supporting Information

**Dual-Quenched and Redox-Responsive Gold Nanoplatforms for Tumor-Specific Multimodal Theranostics**

*Wen Zhou, Nana Wang, Chao Wang, Huangchengzhi Zhang, Zhiwei Xu, Yuxin Huang, Yuyan Zhang, Chen Xie*, Quli Fan**

W. Zhou, N.-N. Wang, C. Wang, H.-C.-Z Zhang, Z.-W. Xu, Y.-X Huang, C. Xie, Q.-L. Fan
State Key Laboratory of Flexible Electronics (LoFE) & Institute of Advanced Materials (IAM)
Nanjing University of Posts & Telecommunications
9 Wenyuan Road, Nanjing 210023, China
E-mail: iamcxie@njupt.edu.cn; iamqlfan@njupt.edu.cn

Y.-Y. Zhang
The Prevention and Control Center for the Geological Disaster of Henan Geological Bureau
28 Jinshui Road, Zhengzhou 450012, China

## 1. Experimental section

**1.1 Chemicals and Materials.** Gold(III) chloride trihydrate and silver nitrate were purchased from Sigma. Diethylenetriaminepentaacetic acid (DTPA) dianhydride was obtained from Shanghai Aladdin. Bis(2-hydroxyethyl) disulfide was purchased from Energy Chemical. Triethylamine (TEA), cetyltrimethylammonium bromide (CTAB), ascorbic acid (AA), and 4-dimethylaminopyridine (DMAP) were obtained from Shanghai Maikelin. Anhydrous $CuSO_4$, N,N'-diisopropylcarbodiimide (DIC), and fetal bovine serum (FBS) were purchased from MERYER. DMEM, phosphate buffered saline (PBS, 1×), calcein-AM and propidium iodide (PI) were purchased from Jiangsu KeyGEN Biotech Corp. Ltd. 1,3-Diphenylisobenzofuran (DPBF), $CuCl_2 \cdot H_2O$, and methanol were purchased from J&K Chemicals Inc. Propargylamine was obtained from Leyan. $mPEG_{5k}$-SH and $N_3$-$PEG_{1k}$-SH were purchased from Ponsure. Methylene blue was obtained from RHAWN. Hydrochloric acid (12 M) and concentrated nitric acid were purchased from Shanghai Hushi Laboratorial Equipment Co., Ltd. Pheophorbide a (PPa), amino acids, including glycine, phenylalanine, arginine, valine, tyrosine, serine, histidine, threonine, proline, tryptophan, aspartic acid, homocysteine, and cysteine, as well as glutathione (GSH), were used as received from Shanghai Yuanye.

**1.2 Characterizations.** Proton nuclear magnetic resonance ($^1$H NMR) spectra were obtained using a Bruker Ultra Shield Plus 400 MHz Spectrometer, with MeOD as solvent. Matrix-assisted laser desorption/ionization time-of-flight (MALDI-TOF) mass spectrometry was conducted on a Bruker Autoflex TOF/TOF spectrometer. Transmission electron microscopy (TEM) images were acquired on a Hitachi HT7700 operated at 100 kV. HAADF imaging and elemental mapping were performed on a Thermo Fisher Scientific FEI Talos 200X at an accelerating voltage of 200 kV. Dynamic light scattering (DLS) and zeta potential measurements were performed on a NanoBrook ZetaPALS Potential Analyzer. UV-vis spectra were recorded with a Shimadzu UV-3600 plus ultraviolet-visible-near-infrared spectrophotometer. Fluorescence spectra were acquired using a Shimadzu RF-6000 plus fluorescence spectrometer. Confocal fluorescence imaging was conducted with a Carl Zeiss LSM880 confocal laser scanning microscope. Flow cytometry analysis was performed using a FlowSight Imaging Flow Cytometer (Merck Millipore, Darmstadt, Germany). PA imaging was carried out using an *in vivo* 3D optoacoustic imaging system (TomoWave Laboratories, Inc.). Thermal images and temperature measurements were obtained with a FLIR E95 thermal imager. Proliferating Cell Nuclear Antigen staining (PCNA) staining, Hematoxylin and Eosin (H&E) staining, and animal experiments were conducted in accordance with the guidelines set by the Laboratory Animal Center of Jiangsu KeyGEN Biotech Corp., Ltd, and approved by the

Animal Ethics Committee of Simcere BioTech Corp., Ltd.

**1.3 Synthesis of Compound 1.** Compound 1 was synthesized via esterification, as outlined in Supplementary Scheme 1. Briefly, PPa (53.4 mg, 0.1 mmol), bis(2-hydroxyethyl) disulfide (46.2 mg, 0.3 mmol), 4-dimethylaminopyridine (14.6 mg, 0.12 mmol), and N, N'-diisopropylcarbodiimide (15.1 mg, 0.12 mmol) were dissolved in anhydrous THF (5.0 mL) in a round-bottom flask. The mixture was stirred at room temperature for 12 hours. Afterward, the solvent was removed under reduced pressure via distillation, and the product was purified by silica gel chromatography. The purified product was concentrated using rotary evaporation, then freeze-dried overnight. Compound 1 (50.0 mg, 74.7 % yield) was obtained and used directly for the next step. MALDI-TOF-MS: m/z calcd. 668.87; found, 670.58 $[M + H]^{+1}$. $^{1}H$ NMR (400 MHz, Methanol-d4) δ: 9.03 (d, 2H), 8.62 (s, 1H), 7.94 (dd, 1H), 6.25 (d, 1H), 6.16 (d, 1H), 5.20 (d, 1H), 5.02 (d, 1H), 4.61 (s, 3H), 4.44 (t, 2H), 4.32 (m, 2H), 3.88 (t, 2H), 3.45 (s, 2H), 3.29 (s, 3H), 3.36 (s, 3H), 2.97 (s, 3H), 2.66-2.53 (m, 2H), 2.51-2.41 (m, 2H), 2.35-2.28 (m, 2H), 2.22-2.12 (m, 3H)

**1.4 Synthesis of Compound 2.** Compound 2 was synthesized through esterification reaction, followed by substitution reaction. In the first step, compound 1 (50 mg, 0.07 mmol) and DTPA dianhydride (178.6 mg, 0.5 mmol) were added to a solvent mixture of TEA (0.2 mL) and DMF (5 mL) and stirred at room temperature for 12 hours. In the second step, propylamine (13.77 mg, 0.25 mmol) was introduced, and the reaction was allowed to proceed for an additional 12 hours at room temperature. After the reaction, the solvent was removed under reduced pressure, and the crude product was purified by HPLC. The purified product was concentrated using rotary evaporation and lyophilized overnight. Compound 2 (45.4 mg, 60.0 % yield) was obtained and used for further use.

**1.5 Synthesis of Cu-PPa.** Compound 2 reacted with copper ions from $CuCl_2$ in a 1:5 molar ratio. The mixture was stirred for 24 hours, followed by 24 hours of dialysis. The final product Cu-PPa was obtained by lyophilization.

**1.6 Synthesis of AuNRs.** AuNRs were synthesized via a seed-mediated growth protocol.[1] Seed solution preparation: CTAB (5 mL, 0.20 M) was combined with $HAuCl_4$ (5.0 mL 0.5 mM) under continuous magnetic stirring (450 rpm). To initiate nucleation, 0.60 mL of ice-cold 0.01 M $NaBH_4$ was rapidly added under vigorous stirring (1450 rpm), yielding a brownish-yellow colloidal suspension. The seed solution was aged at 25 °C for 2 h. AuNRs growth: a growth solution was prepared by sequentially mixing CTAB (10 mL, 0.20 M), $AgNO_3$ (4 mM, 0.3 mL) and $HAuCl_4$ (10 mL, 1 mM) at 28 °C under mild stirring (450 rpm). Ascorbic acid (140 μL, 0.0788 M) was introduced, resulting in a colorless solution. Subsequently, 24 μL of seed

solution was dropwise infused into the growth medium under gentle agitation (450 rpm). The color of the solution gradually turned wine red within 20 minutes. The mixture was then aged for 12 h at 28 °C. Residual CTAB and byproducts were removed via two centrifugation cycles (8,000 g, 30 min), and the purified AuNRs were stored in aqueous suspension.

**1.7 PEGylation of Gold Nanorods.** CTAB surfactants on AuNRs surfaces were replaced with heterofunctional polyethylene glycol (PEG) derivatives. A mixed PEG-thiol solution (0.2 mM) containing mPEG5k-SH (80 mol%) and $N_3$-PEG1k-SH (20 mol%) was prepared to enable subsequent biofunctionalization. The CTAB-capped AuNRs dispersion was combined with an equal volume of PEG solution and incubated for 2 h at 25 °C under stirring, facilitating thiol-gold coordination. Unbound PEG molecules were eliminated through triple centrifugation (8,000 g, 15 min), and the PEGylated AuNRs (AuNRs-PEG) were redispersed in Milli-Q water.[2]

**1.8 Fabrication of AuPPCs.** Azide-functionalized AuNRs-PEG were conjugated with alkyne-terminated Cu-PPa via copper(I)-catalyzed azide-alkyne cycloaddition (CuAAC). Cu-PPa (0.4 mg/mL, 1 mL) was introduced into AuNRs-PEG, followed by the addition of sodium ascorbate (100 μL, 7.5 mg/mL). Then, rapidly inject $CuSO_4$ (10 μL, 3 mg/mL) to initiate the click reaction. The mixture was purged with $N_2$ and stirred for 18 h in the dark. Unreacted reagents were removed by triple centrifugation (8,000 g, 30 min).

**1.9 Characterization of Gold Nanorods.** Extinction spectra were collected from AuNRs, AuNRs-PEG, and AuPPCs in a Shimadzu UV-3600 plus ultraviolet-visible-near-infrared spectrophotometer at room temperature with 1 cm of optical path. The fluorescent spectra of AuNRs-PEG, PPa and AuPPCs solutions were characterized by a Shimadzu RF-6000 plus fluorescence spectrometer. The DLS sizes and zeta potentials of the AuNRs, AuNRs-PEG, and AuPPCs on a NanoBrook ZetaPALS Potential Analyzer. The shape and morphology of the AuNRs were assessed with transmission electron microscopy (TEM) imaging (a Hitachi HT7700 TEM, operated at 100 kV). The size distribution of the AuNRs was calculated using Image J. HAADF image and elemental maps of AuPPCs were charaterized on a Thermo Fisher Scientific FEI Talos (operated at 200 kV).

**1.10 Quantification of PPa Conjugation Efficiency on AuNRs-PEG Nanoparticles & Photostability of AuPPCs.** The amount of Cu-PPa conjugated to PEGylated gold nanorods (AuNRs-PEG) was ascertained by quantifying the difference between the total and free Cu-PPa concentrations in the conjugation mixture. Specifically, AuNRs-PEG nanoparticles with an optical density (OD) of 3 were incubated with Cu-PPa at a concentration of 0.4 mg/mL, following the aforementioned procedure. Subsequently, the mixture underwent centrifugation

to separate the conjugated nanoparticles from the unbound Cu-PPa, and the supernatant containing the excess ligand was carefully collected. In tandem, a set of Cu-PPa standard solutions was prepared, encompassing a range of concentrations that bracketed the expected levels in the supernatants. These standards were formulated under conditions that mirrored those of the supernatant samples to ensure comparability. The fluorescence intensity of both the standards and the supernatants was then measured using a Shimadzu RF-6000 plus fluorescence spectrometer, with an emission wavelength of 665 nm, characteristic of the Cu-PPa fluorophore. By subtracting the concentration of free Cu-PPa from the total amount initially added to the conjugation reaction, the amount of Cu-PPa successfully conjugated to the AuNRs-PEG nanoparticles was calculated.

The photostability of AuPPCs was evaluated under continuous laser irradiation for 0, 1, 2, 3, 4, 5, and 6 min (635 nm, 0.1 W/cm$^2$). Subsequently, the fluorescence intensities at different irradiation durations were measured using a Shimadzu RF-6000 Plus fluorescence spectrometer.

**1.11 GSH-Responsiveness and Selectivity Assay of AuPPCs**

Varying concentrations of GSH (0, 0.4, 0.8, 1.2, and 1.6 mM) were incubated with AuPPCs (6.0 μg/mL) in PBS containing 1 mg/mL BSA at 37 °C for 30 min, followed by fluorescence and UV–vis measurements. To evaluate selectivity, AuPPCs were separately incubated with blank PBS or different amino acids, including glycine, phenylalanine, arginine, valine, tyrosine, serine, histidine, threonine, proline, tryptophan, aspartic acid, homocysteine, cysteine, and GSH, under identical conditions. The fluorescence intensities were then recorded to assess the selective response of the nanoprobes toward GSH.

**1.12 Measurement of singlet oxygen generation.** To measure $^1O_2$ generation of AuPPCs under 635 nm laser irradiation, the absorption loss of DPBF is monitored. In this process, DPBF is introduced into a solution containing either Cu-PPa or AuPPCs, both at 6 μg/mL, with 20 μg/mL BSA present, with or without GSH (1.6 mM). The obtained mixture is then subjected to 635 nm laser irradiation at an intensity of 0.1 W/cm$^2$. At various time points during irradiation, the UV-vis absorbance spectra of the solution, or specifically the absorbance at 414 nm (the characteristic absorption peak of DPBF), are recorded.

**1.13 Hydroxyl radical (•OH) detection.** Methylene Blue (MB) was utilized as an indicator for •OH detection. In the MB-based method, an AuPPCs solution (6 μg/mL) was mixed with GSH (1.6 mM), $H_2O_2$ (10 mM), and 20 μg/mL of MB in the presence of 20 μg/mL BSA. The absorption spectra of the five samples were recorded: 1) AuPPCs + MB; 2) AuPPCs + MB + $H_2O_2$; 3) AuPPCs + MB + GSH; 4) AuPPCs + MB + $H_2O_2$ + GSH (0.8 mM); 5) AuPPCs + MB

+ $H_2O_2$ + GSH (1.6 mM).

**1.14 Photothermal effect.** AuPPCs (200 μL) of varying concentrations (31.25, 62.5, 125, 250, 500 μg/mL) were irradiated with a 635 nm laser for different durations, followed by natural cooling to room temperature. The temperature of the solution was monitored throughout the process using a thermal camera. The heating and cooling cycles were performed using 500 μg/mL AuPPCs, where each cycle consisted of a 10-minute irradiation with a 635 nm laser at 1 W/cm$^2$, followed by a 10-minute natural cooling period.

**1.15 Cellular uptake.** The release of PPa from the surface of AuPPCs imparts them with red fluorescence, facilitating their application in confocal imaging. Murine breast carcinoma 4T1 cells, procured from Jiangsu KeyGEN Biotech Corp. Ltd. were propagated in Dulbecco's modified Eagle's medium (DMEM) supplemented with 10% fetal bovine serum (FBS) and antibiotics (10 mg/mL of streptomycin and 10 U/mL of penicillin), and maintained in an environment comprising 5% carbon dioxide ($CO_2$) and 95% humidified air at 37°C. Subsequently, the cells were seeded into confocal dishes for 24 h, after which AuPPCs were added. After incubation periods of varying durations, the cells were rinsed with fresh DMEM, and their nuclei were stained with DAPI. Confocal images were then acquired under excitation wavelengths of 405 nm for DAPI and 632 nm for AuPPCs, respectively. For flow cytometry analysis, 4T1 cells were seeded into 12-well cell culture plates at a density of $2\times10^5$ cells per well and incubated for 1, 3, 6, or 9 h. Following incubation, the cells were washed with PBS, trypsinized, collected into 5 mL tubes, and their fluorescence was quantified using a FlowSight imaging flow cytometer.

**1.16 Cytotoxicity assay (MTT) and live/dead cell staining analysis.** Cytotoxicity evaluation utilizing the MTT assay and live/dead cell staining analysis was conducted on 4T1 cells. The cells were seeded into 96-well plates at a density of 10,000 cells per well in 100 μL of medium and incubated for 24 hours to allow for cell attachment and growth. Subsequently, AuPPCs were diluted to various concentrations (0, 1, 2, 4, 8, 16, and 32 μg/mL) in fresh medium and added to the cells. Following a 12-hour incubation period, a subset of the 4T1 cells were exposed to 635 nm laser irradiation at a power density of 0.1 W/cm$^2$ for 5 minutes, while the remaining cells served as controls without laser treatment. After an additional 12-hour incubation, the relative cell viabilities were assessed using the standard MTT assay. Specifically, the medium was replaced with fresh medium containing MTT (20 μL at 5 mg/mL), and the plates were incubated for another 4 hours. The medium was then aspirated, and 100 μL of DMSO was added to each well. The plates were vigorously shaken for 5 minutes at room temperature to ensure complete solubilization of the MTT formazan crystals. The absorbance

of the cells at 490 nm was measured using a microplate reader, and cell viability was calculated as the ratio of the absorbance of the cells treated with AuPPCs to that of the untreated control cells.

To visualize the viability of the nanoprobe-treated cells after laser irradiation, live/dead cell staining was performed using calcein-AM and propidium iodide (PI). Briefly, following the same treatment protocol as described above, the cells were incubated with either PBS (control) or AuPPCs, with or without laser irradiation. Subsequently, fresh medium containing calcein-AM and PI was added to the cells, and the plates were incubated in the dark at 37°C for 30 minutes. After washing the cells with phenol red-free medium, images were captured using a Carl Zeiss LSM880 confocal laser scanning microscope.

**1.17 Apoptosis evaluation by flow cytometry.** 4T1 cells (~ $5\times10^5$) were seeded into 6-well plates and incubated at 37 $^oC$ for 24 h, and the cells were randomly divided into four groups, which were (1) PBS, (2) PBS + laser, (3) AuPPCs, (4) AuPPCs + laser. The cells were incubated with PBS or AuPPCs for 12 h, followed by laser irradiation or not for 5 min (0.1 W/$cm^2$). Then, cells were incubated at 37 $^oC$ for 12 h. After incubation, the medium was removed, the cells were washed with PBS, and fresh culture medium was added. After removal of the medium, the cells were trypsinized, collected, and resuspended in 1 mL PBS, and stained with Annexin V-FITC/PI. After staining, the apoptotic cell population was analyzed using a Flow Sight Imaging Flow Cytometer.

**1.18 Intracellular ROS detection.** 4T1 cells and NIH 3T3 cells were separately seeded into confocal dishes and cultured for 24 h. Serum-free DMEM and AuPPCs (32 μg/mL) were then added to the dishes and cultured for 3 h. After that, DCFH-DA (20 μM) was added, then the cells were irradiated under 635 nm for 0, 1, 2, and 3 min, separately. The confocal fluorescence images were captured under excitation at 488 nm.

**1.19 Cellular chemodynamic ˙OH detection.** After replacing the culture medium with fresh DMEM, 4T1 and NIH 3T3 cells were treated with AuPPCs (32 μg/mL) for 3 h. Subsequently, the medium was removed, and cells were thoroughly washed with PBS (3 × 5 min). The cells were then subjected to different incubation with DCFH-DA (0, 10, 20, and 30 min) under culture conditions. Intracellular hydroxyl radical generation was imaged by monitoring the fluorescence using confocal laser scanning microscope.

**1.20 Tumor mouse model.** All experimental procedures involving animals were conducted in compliance with the institutional guidelines established by the Laboratory Animal Center of Jiangsu KeyGEN Biotech Corp., Ltd. (Approval No. IACUC-007), with ethical review and approval obtained from the Animal Ethics Committee of Simcere BioTech Corp. Ltd. To

establish subcutaneous tumor models, female BALB/c mice (6-8 weeks old) received unilateral implantation of $1\times10^6$ 4T1 murine mammary carcinoma cells in the left axillary region through subcutaneous injection. Tumor dimensions were measured using digital calipers, and tumor volume (V) was calculated using the ellipsoid approximation formula: $V = (D \times d^2)/2$, where D represents the major axis (longest diameter) and d denotes the minor axis (shortest perpendicular diameter) of the neoplastic growth.

**1.21 In vivo anticancer study.** 4T1 tumor-bearing mice were randomly stratified into four experimental cohorts (n=5/group) using randomization: 1) PBS control, 2) AuPPCs monotherapy, 3) PBS + laser phototherapy, 4) AuPPCs + laser combination therapy. Each group was injected with phosphate-buffered saline or AuPPCs nanoparticles (100 μL, 50 μg/mL) intravenously. The photo-mediated intervention was performed using a 635 nm diode laser (fluence rate: 0.3 W/cm$^2$) applied transcutaneously to neoplastic lesions for 20 minutes at 8 h post-injection. The groups with laser irradiation were subjected to whole-body thermal imaging of mice, and the tumor site temperature was recorded. To evaluate the therapeutic efficacy, tumor volume and body weight were measured every two days. Terminal procedures on day 14 post-treatment included necropsy with subsequent histopathological evaluation, which were conducted as follows: a) PCNA immunohistochemical staining of excised tumors across all groups, b) H&E morphological analysis of major organs from combination therapy mice. c) blood biochemistry analysis.

**1.22 Data analysis**

Statistical calculations were performed using GraphPad Prism software. Data are presented as mean ± SD unless otherwise mentioned. For continuous variables, between-group differences were analyzed using: (1) two-tailed Student's t-test for dual-group comparisons, or (2) one-way ANOVA with Tukey's post hoc tests for multi-group comparisons (≥3 groups). Statistical significance was defined as $p < 0.05$.

## 2. Supporting figures

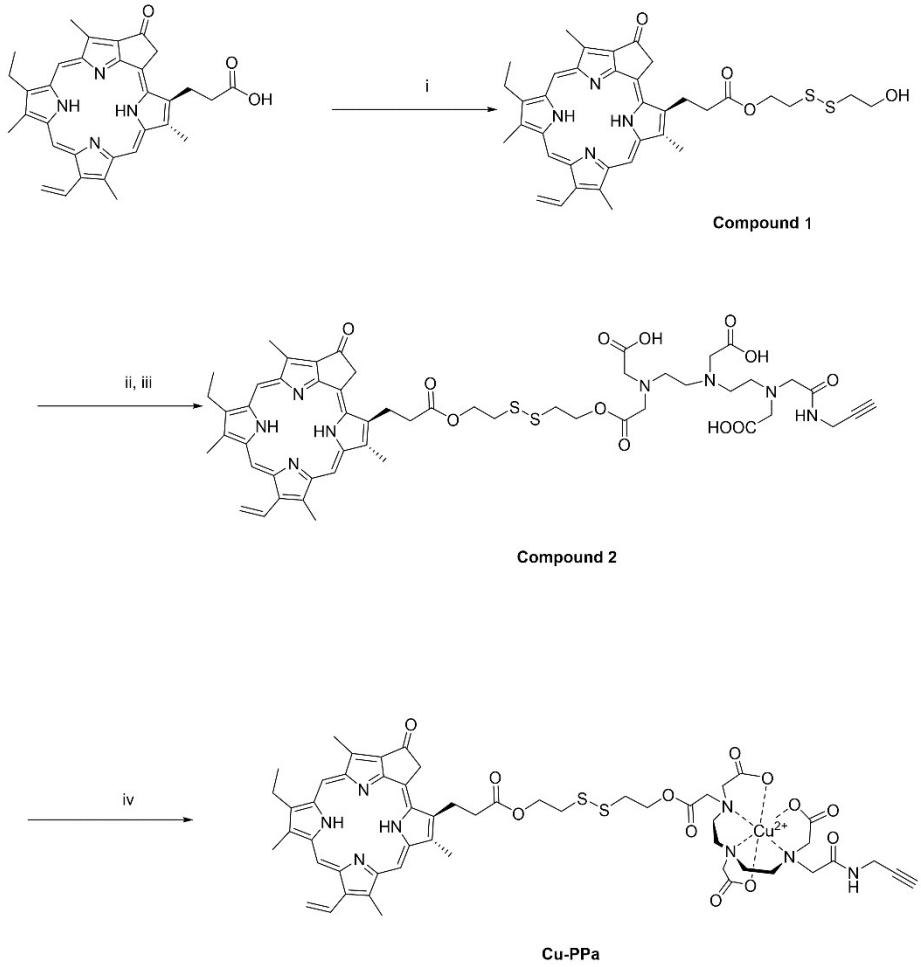


**Figure S1.** Synthetic route of Cu-PPa. (i) PPa, bis(2-hydroxyethyl) disulfide, DIC, DMAP, anhydrous DMF, RT, 24 h. (ii) DTPA dianhydride, TEA, anhydrous DMF, RT, 12 h. (iii) Propargylamine, RT, 12 h. (iv) $CuCl_2$, $H_2O$, RT, 24 h.

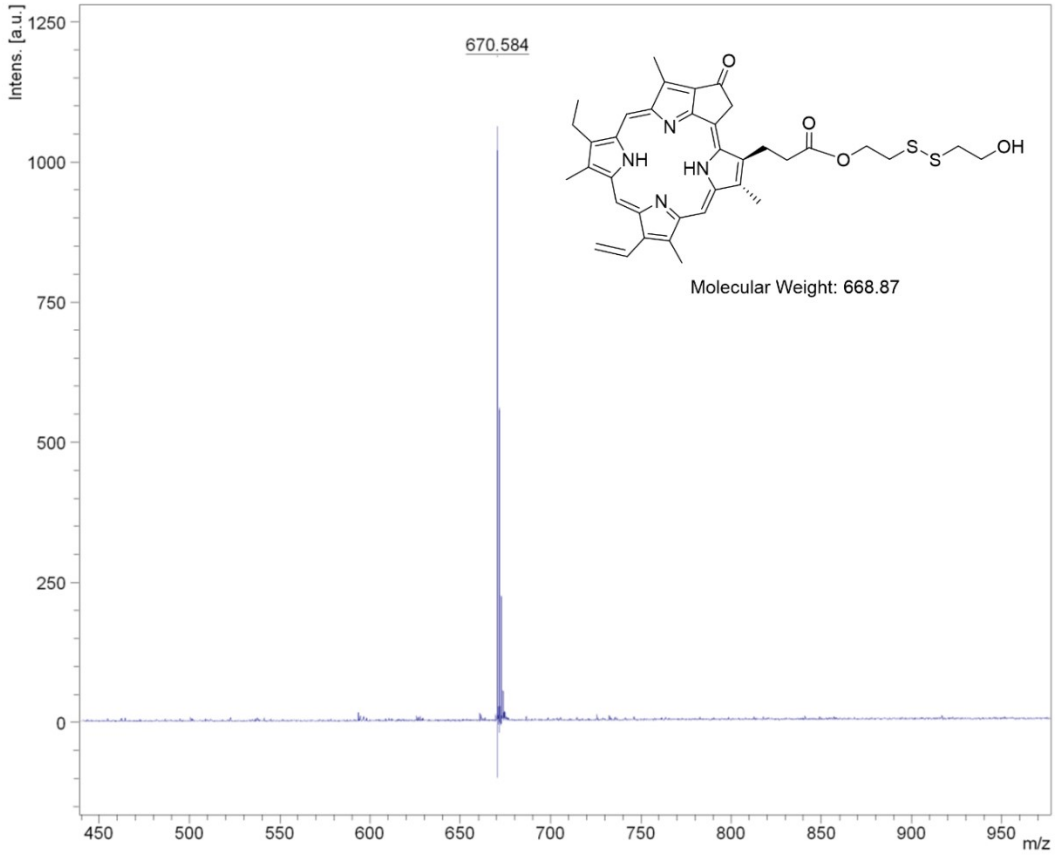


**Figure S2.** MALDI-TOF MS spectrum of compound 1.

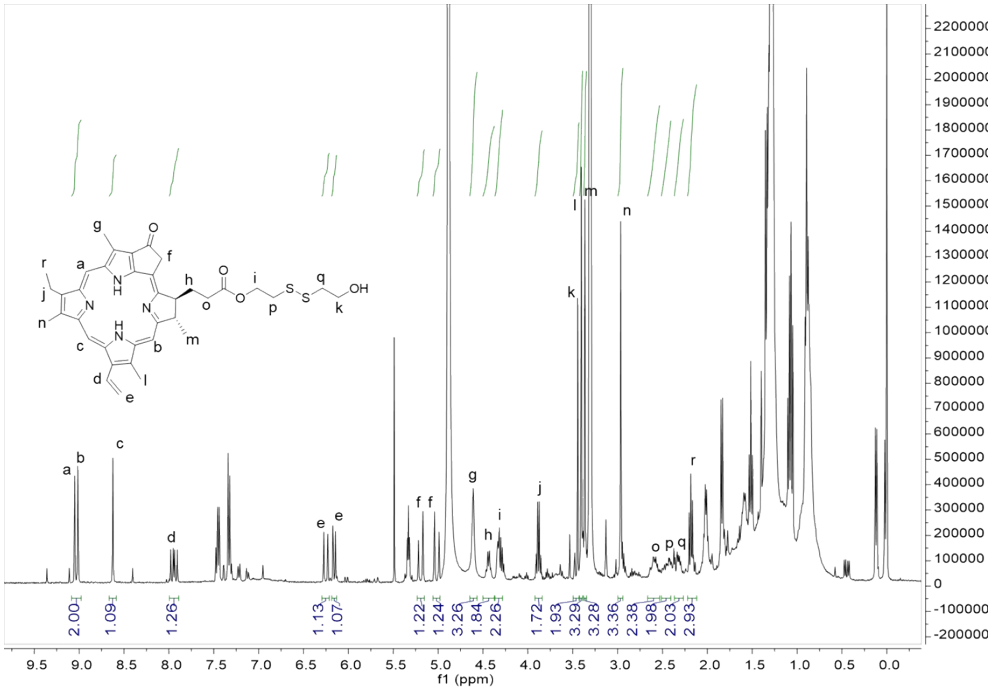


**Figure S3.** [1]H NMR spectrum of Compound 1. Solvent: MeOD.

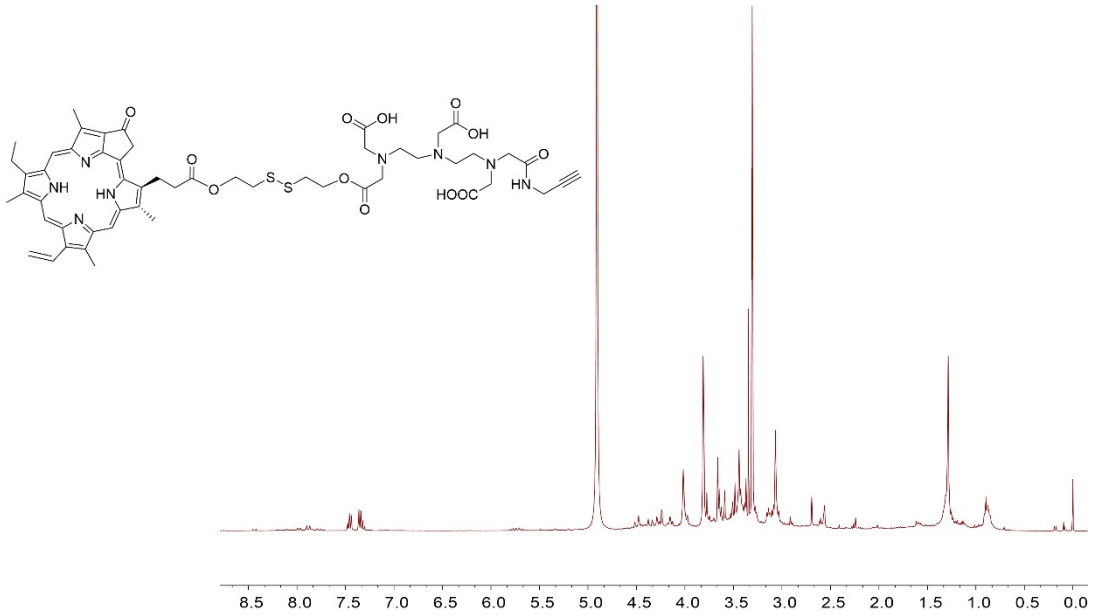


**Figure S4.** $^{1}$H NMR spectrum of pheophorbide a-ethyl disulfide diethylenetriaminepentaacetic propargylamine alkyne (compound 2). Solvent: MeOD.

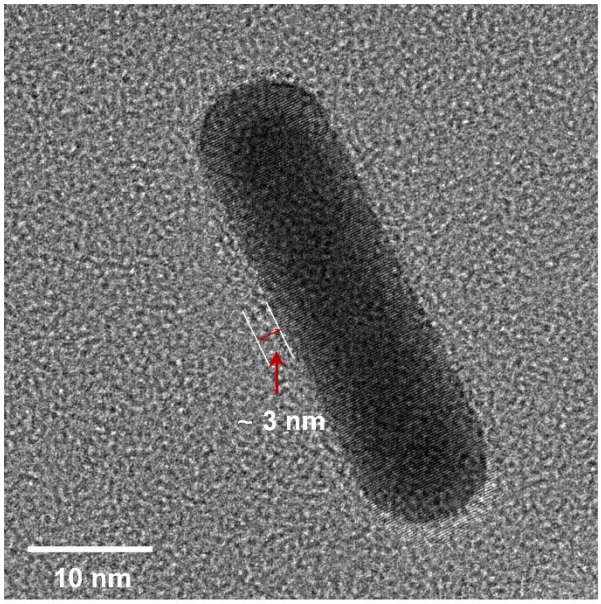


**Figure S5.** TEM image of AuPPCs coated with an organic shell about 3 nm thick.

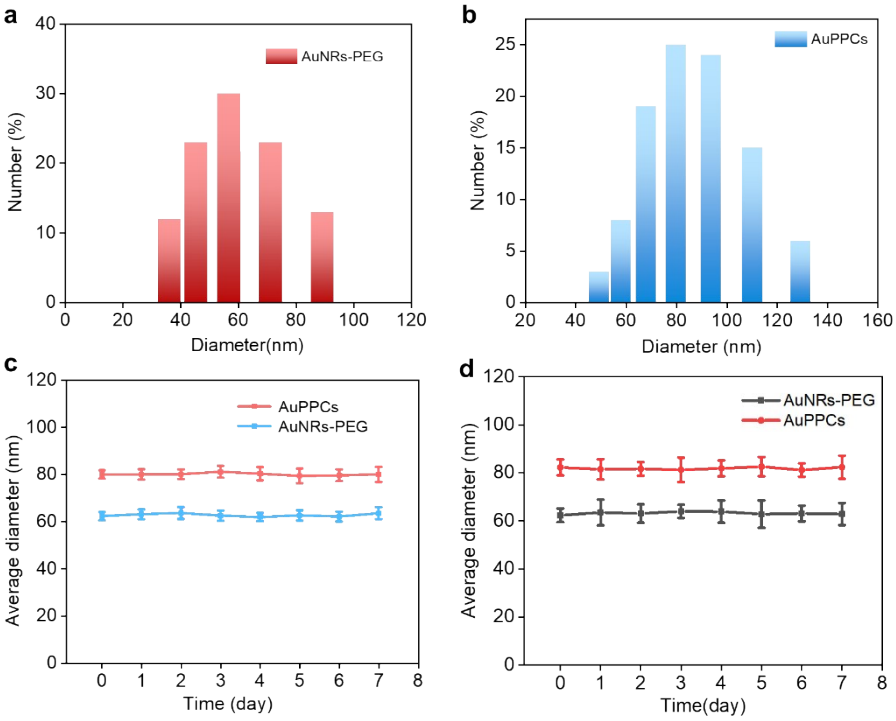


**Figure S6.** Hydrodynamic size distribution of a) AuNRs-PEG and b) AuPPCs in serum-containing medium. The stability of AuNRs-PEG and AuPPCs in c) 1 × PBS, d) serum-containing medium.

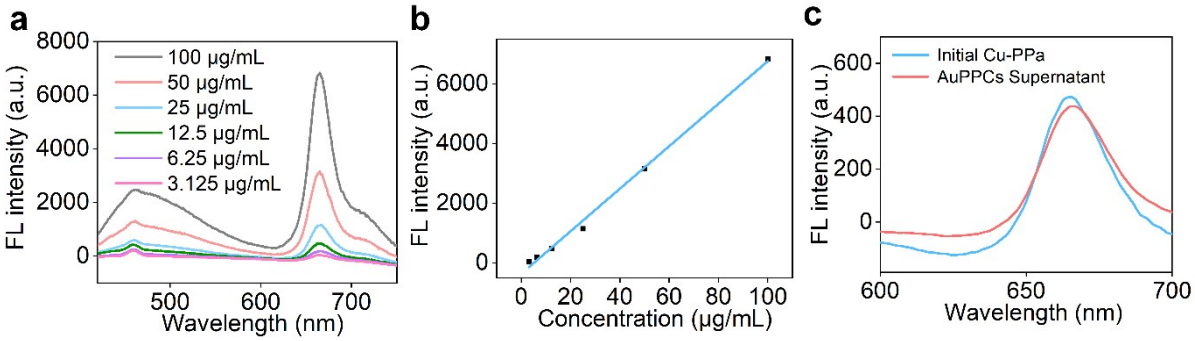


**Figure S7.** Quantification of Cu-PPa reacting with AuNRs-PEG using FL. a) The FL spectra of different concentrations of Cu-PPa. b) The standard curve of Cu-PPa based on FL. c) The FL spectra of the initial and supernatant of the reaction of Cu-PPa with AuNRs-PEG.

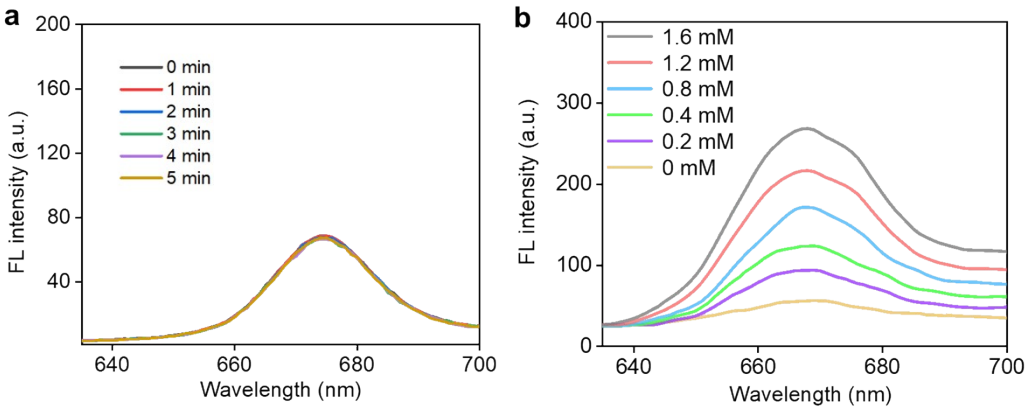


**Figure S8.** FL spectra of the AuPPCs. a) Photostability of AuPPCs under continuous laser irradiation for 0, 1, 2, 3, 4, 5, and 6 min (635 nm, 0.1 W/cm$^2$). b) FL spectra of AuPPCs after incubation with different concentrations of GSH.

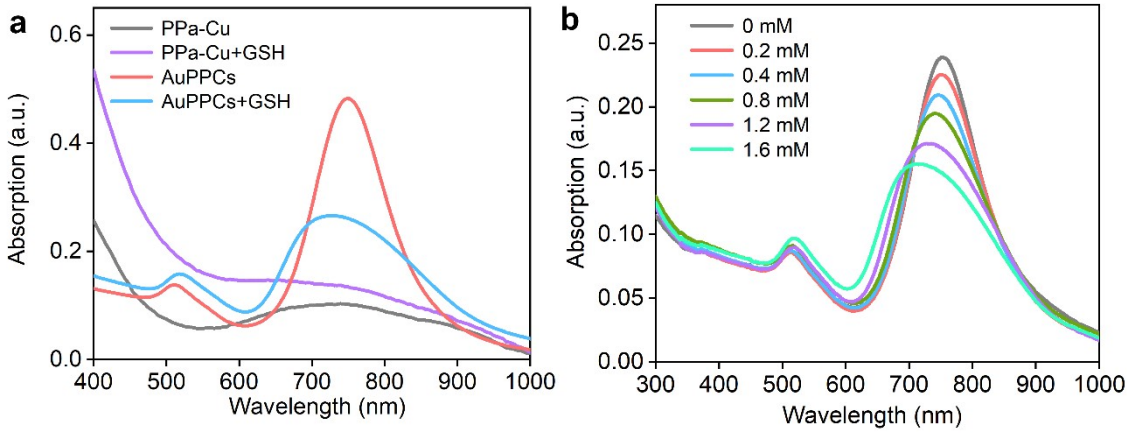


**Figure S9.** a) UV-vis spectra of Cu-PPa and AuPPCs incubated with or without 1.6 mM GSH in 20 μg/mL BSA, respectively. b) UV-vis spectra of AuPPCs incubated with different concentrations of GSH at 37 °C for 30 min.

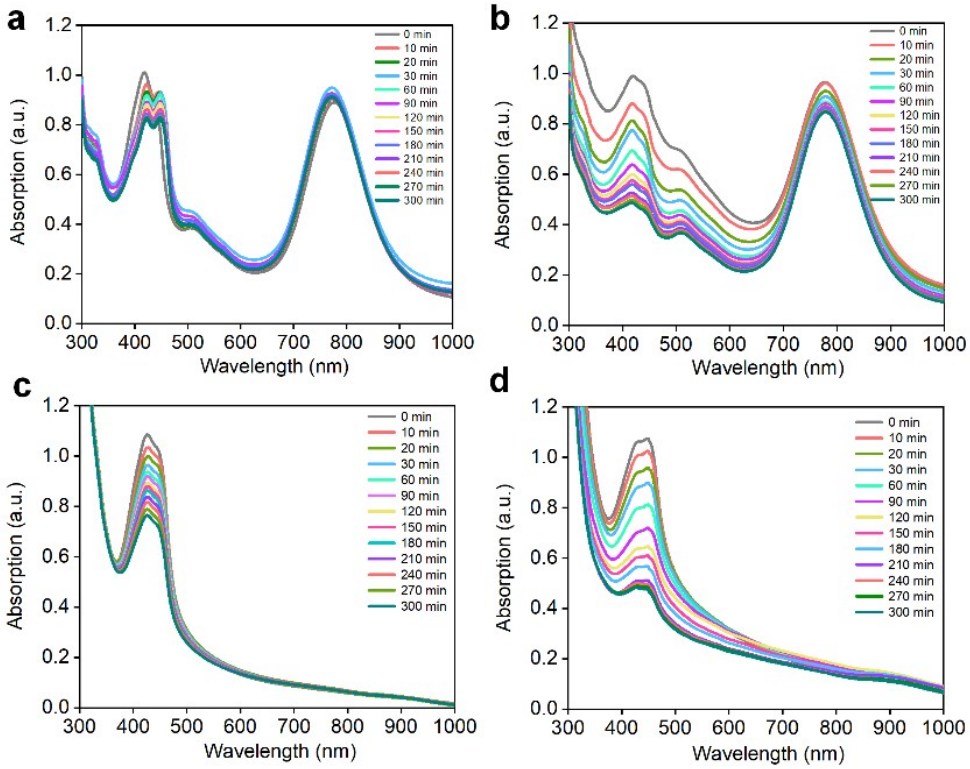


**Figure S10.** Absorption changes of DPBF incubated with a) 6 μg/mL AuPPC without GSH. b) 6 μg/mL AuPPC with 1.6 mM GSH. c) PPa-Cu 6 μg/mL without GSH. d) 6 μg/mL PPa-Cu with 1.6 mM GSH with time under 635 nm laser irradiation (0.1 W/cm$^2$, 5 min). All experiments are conducted in 20 μg/mL BSA.

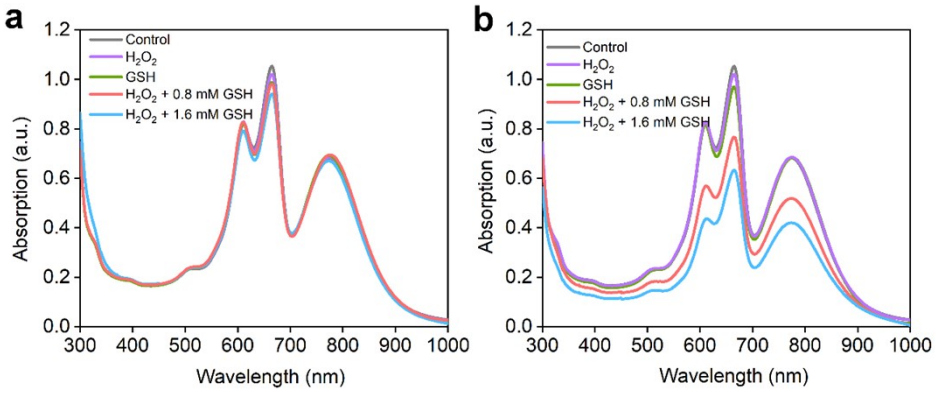


**Figure S11.** Absorption spectra of MB (20 μg/mL) under treatment with AuPPCs (6 μg/mL) and $H_2O_2$ (10 mM) at varying GSH concentrations in the presence of BSA (1 mg/mL), recorded at a) 0 min and b) 30 min.

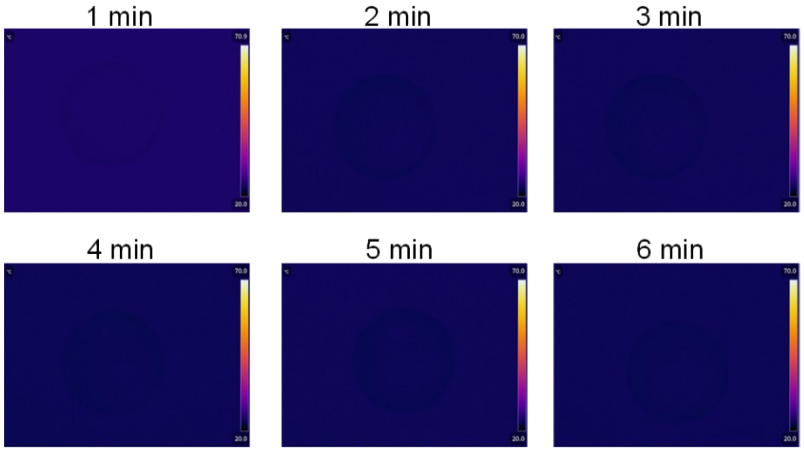


**Figure S12.** Representative IR thermal images of 4T1 cells under 635 nm laser irradiation at different time points: 0, 1, 2, 3, 4, 5, and 6 minutes (0.1 W/cm$^2$).

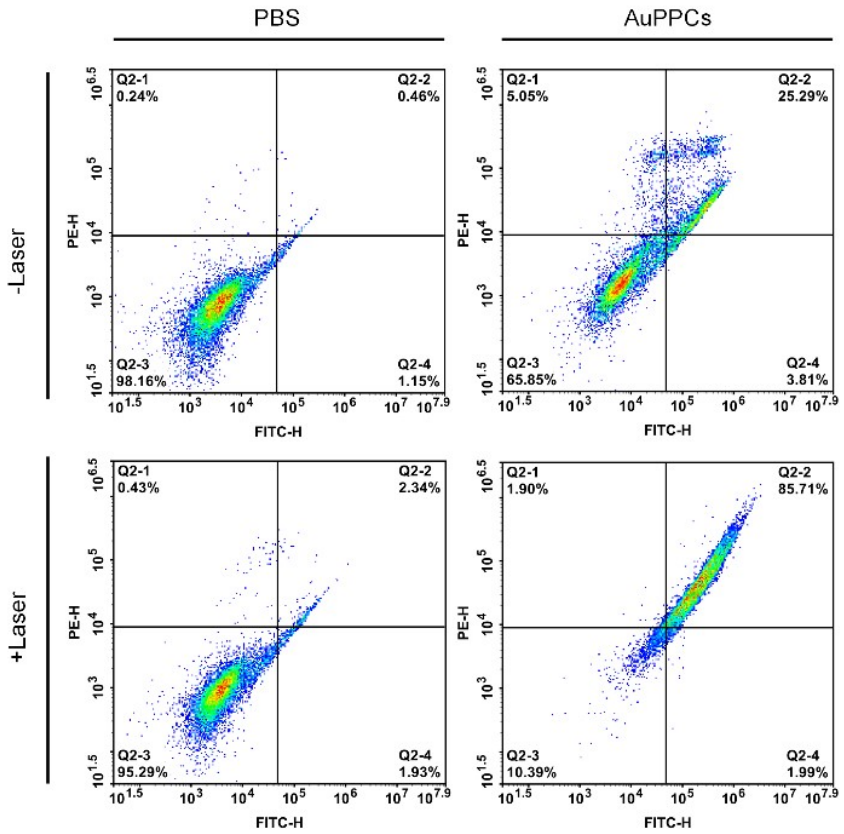


**Figure S13.** Flow cytometry analysis of 4T1 cell viability after treatment with PBS or AuPPCs, with or without 635 nm laser irradiation (0.1 W/cm$^2$, 5 min).

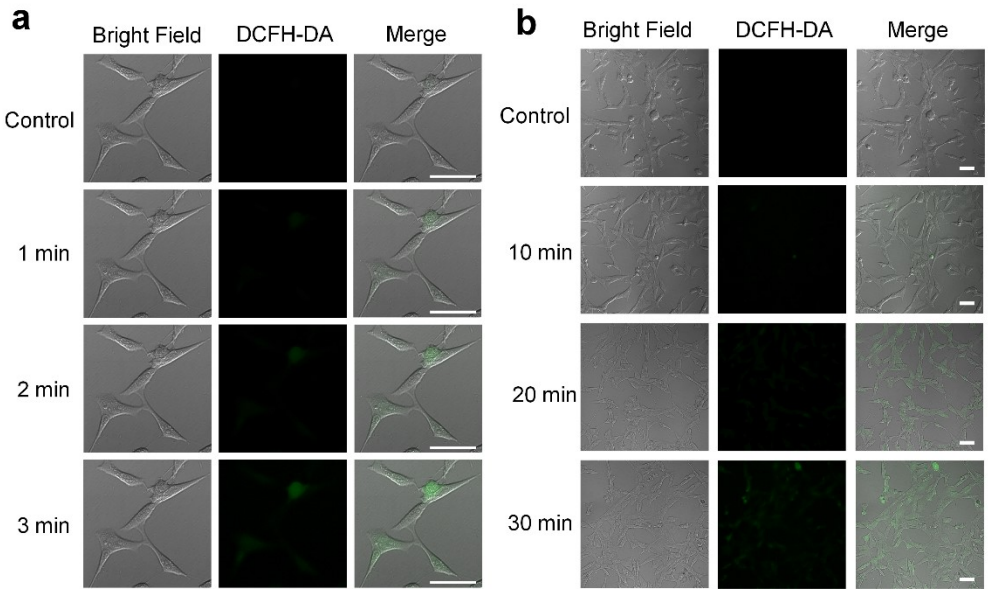


**Figure S14.** Confocal fluorescence images of NIH-3T3 cells incubated with AuPPCs for 3 hours, followed by 15-minute incubation with DCFH-DA. a) PDT study: Cells subjected to 635 nm laser irradiation (0.1 W/cm$^2$) for different durations: 1 min, 2 min, and 3 min. b) CDT study: Cells without laser irradiation, incubated for varying time intervals: 10 min, 20 min, and 30 min.

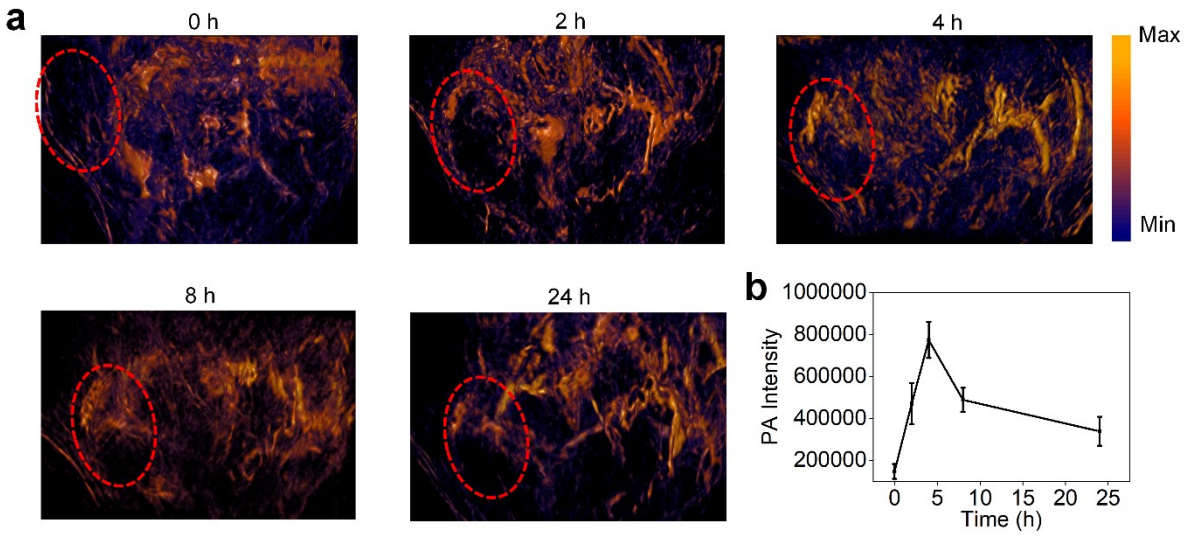


**Figure S15.** Photoacoustic imaging and the corresponding qualification curve of mice as a function of AuPPCs injection time.

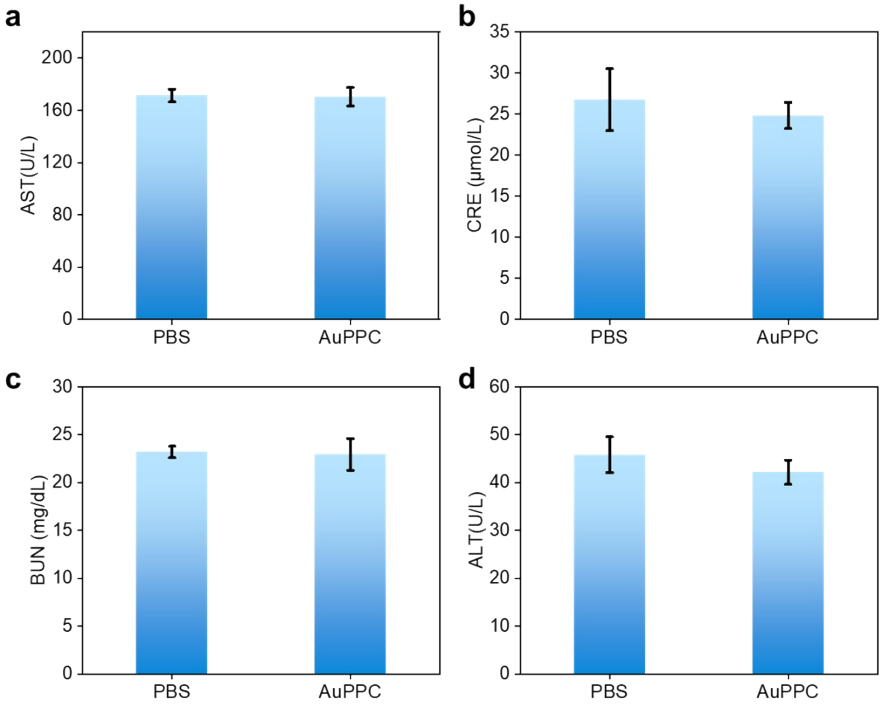


**Figure S16.** Blood biochemical parameters of mice following different treatments. a) Aspartate aminotransferase (AST), b) Creatinine (CRE), c) Blood urea nitrogen (BUN), and d) Alanine aminotransferase (ALT). Data are presented as mean ± SD based on five independent samples (n = 5).

## References

[1] A. Gole, C. J. Murphy, *Chem. Mater.*, **2004**, *16*, 3633.
[2] Y.-S. Chen, Y. Zhao, S. J. Yoon, S. S. Gambhir, S. Emelianov, *Nat. Nanotechnol.,* **2019**, *14*, 465.